JOC The Journal of Organic Chemistry

pubs.acs.org/joc Note

Close Amide NH···F Hydrogen Bonding Interactions in 1,8-Disubstituted Naphthalenes

Muhammad Kazim, Maxime A. Siegler, and Thomas Lectka*

Cite This: J. Org. Chem. 2020, 85, 6195−6200 Read Online

ACCESS | Metrics & More | Article Recommendations | Supporting Information

ABSTRACT: In this note, we present a series of *N*-(8-fluoronaphthalen-1-yl)benzamide derivatives designed to maximize amide-NH···F hydrogen bond interactions therein. A combination of IR and NMR spectroscopy indicates a linear correlation between the high energy shift in NH stretching frequency and the electron withdrawing nature of the substituent, consistent with the trend predicted by DFT calculations. Additionally, a limiting case of hydrogen bonding is observed when the benzamide derivatives are replaced with trifluoroacetamide, causing an additional red shift of 44 cm^{-1} in the NH stretching frequency. Most importantly, $^{1}H-^{19}F$ coupling constants in this series are among the largest measured for amide-NH···F interactions. X-ray crystallography reveals face-to-face alignment of naphthalene rings in these derivatives resulting in part from the NH···F hydrogen bonds. This motif also dictates the formation of sheets composed of stacked naphthalene rings in the crystal structure as opposed to unfluorinated analogues wherein NH···OC hydrogen-bonding interactions force benzamide and naphthalene rings to engage in T-shaped $\pi-\pi$ interactions instead. Additionally, the NH proton in the trifluoroacetamide derivative engages in extended H-bond interactions in its crystal structure.

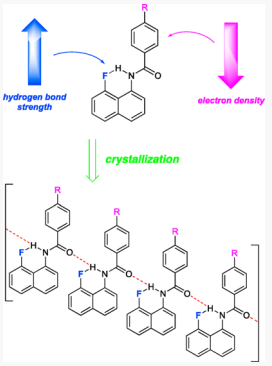

The interaction of C−F bonds, especially in proteins, with proximate functional groups is a topic of lively interest and discussion.[1−6] Their importance in dictating protein structure and function is not yet fully answered, including the dilemma of whether such interactions themselves are due to propinquity, attractive interactions, or a combination thereof. Over the past several years we have investigated close interactions between C−F bonds and common organic functional groups in relatively small molecules that are often dictated by forced proximity, along with some measure of attraction and repulsion.[7−13] The case of the amide NH···F interaction is presumably one of the more interesting, due to the ubiquity of amide residues in proteins. Nevertheless, a search of the Cambridge Crystallographic Database (CCD) indicates only a few substantial interactions; most are self-evidently weak and long-range. The closest such interaction we found was approximately 1.93 Å.[14] We thought it would be illustrative and useful to investigate the closest range and thus strongest model interaction we could conceive in order to achieve a fuller understanding. In this note, we employ the 1,8-disubstituted naphthalene scaffold to investigate a series of amide NH···F interactions that are by spectroscopic measures more intense than those exhibited in the available crystal structure database. Historically, these so-called "proton sponge" derivatives have often been used to investigate the nature of close H-bonding interactions.[15−20] We imagined that a series of these molecules would once again serve as excellent models for the study of amide-NH···F interactions (Figure 1).

Chemical intuition suggests that the *trans*-amide conformation of these *N*-(8-fluoronaphthalen-1-yl)benzamide derivatives would make the N−H proton particularly available to engage in hydrogen bonding to the neighboring "peri" fluorine atom. On the other hand, $\pi-\pi$ interactions in aromatic compounds[21−24] are well-known to skew the rotameric preferences of aryl amides. To shed light on the relative stabilities of the rotamers—and thereby possible H-bonding interactions—we turned to DFT calculations. At ωB97XD/6-311+G**, we located the cis and trans rotamers for each derivative (Figure 2, see Supporting Information "SI" for details). In trans structures **1**−**4**, the NH hydrogen resides at a position maximizing the NH···F interaction, whereas it bends out of the plane of naphthalene ring in cis structures **1a**−**4a**, thus attenuating the interaction (Figure 2). As it were, the desired rotamers were predicted to be

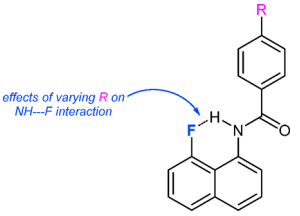

Figure 1. NH···F interaction in *N*-(8-fluoronaphthalen-1-yl)benzamide derivatives.

Received: March 2, 2020
Published: March 31, 2020

https://dx.doi.org/10.1021/acs.joc.0c00553
J. Org. Chem. 2020, 85, 6195−6200

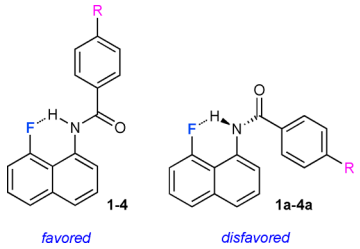

Figure 2. Rotameric forms located by DFT calculations (ωB97XD/6-311+G**) with **1**−**4** favored over **1a**−**4a** by >2.3 kcal/mol.

more stable by at least 2.3 kcal/mol as we would ordinarily expect. Additionally, the amide NH···F distances in the series **1**−**4** are predicted to lie in the range of 1.84−1.86 Å (gas phase), smaller than the shortest distance of 1.93 Å observed crystallographically.[14]

Curiously, replacing the fluorine with hydrogen attenuates the preference for the desired rotamer and no stability trend is observed when test molecules **5** were optimized at the same level of theory (Figure 3, Table S2). In fact, the NH proton bends out

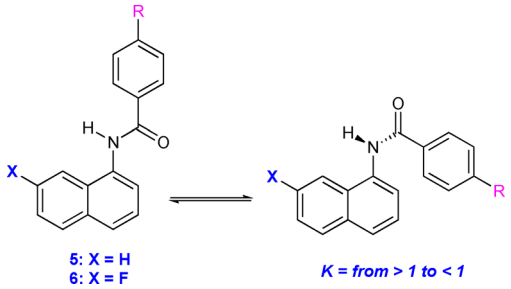

Figure 3. Rotamers of **5** and **6** optimized for rotameric preferences with DFT calculations at ωB97XD/6-311+G**. R = NMe_2, OMe, H, NO_2.

of the plane of the naphthalene ring in both optimized rotamers (see SI). Similarly, no noticeable trend was observed when rotamers of 7-fluoro-1-aminonaphthalene derivatives were optimized (**6**, Figure 3, Table S3). These calculations suggested to us that the relative stability of desired rotamers could be attributed in part to favorable NH···F interactions. Therefore, having a fluorine atom at that position may prove essential to the investigation as it locks the structure in the desired orientation.

After DFT calculations pointed us in the right direction, we synthesized the desired molecules from commercially available 1,8-diaminonaphthalene **8**. Treatment of **8** with isoamyl nitrite followed by HF-pyridine resulted in the formation of 8-fluoro-1-aminonaphthalene **10**,[25] which was then acetylated with a series of substituted benzoyl chlorides to afford *N*-(8-fluoronaphthalen-1-yl)benzamide derivatives in 75−85% yields (Scheme 1). The dimethylamino analogue **4** was synthesized by reduction/alkylation of p-NO_2 derivative **3** (Scheme 1).

The two rotamers can easily be distinguished based on the NH···F spin−spin coupling constants predicted by DFT calculations (B3LYP/6-311++G**). In *trans*-amide conformations, the calculated coupling constants lie between 24 and 27 Hz, whereas for the undesired rotamers as well as rotamers of **5** and **6** those numbers drop to 0−2 Hz. Experimentally, the ^{1}H NMR spectra of all derivatives show NH protons as apparent doublets (J_{H-F} = 20−21 Hz). On the other hand, the ^{19}F NMR spectra reveal complex multiplets (see SI). Both ^{1}H and ^{19}F NMR spectra indicate that the products of Scheme 1 are locked exclusively in the desired *trans* orientation. The ^{19}F NMR of all

Scheme 1. Synthesis of *N*-(8-Fluoronahphthalen-1-yl) Benzamide Derivatives

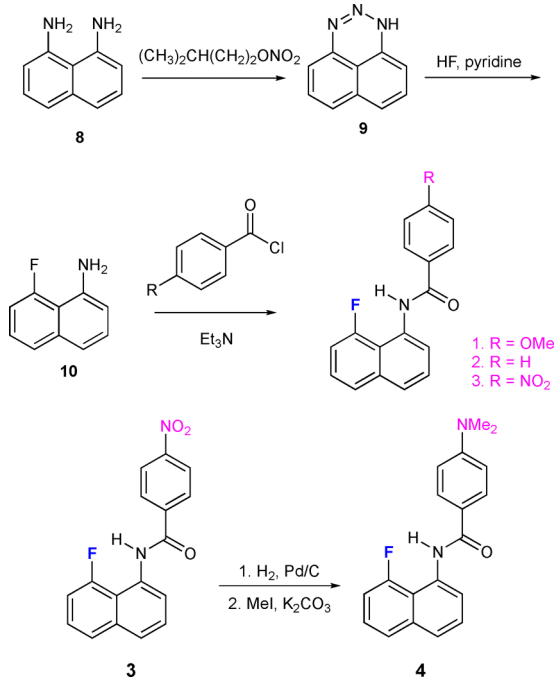

the derivatives also reveal consistent 16 Hz coupling constants corresponding to the interaction of the F nucleus with the ortho proton on the naphthalene ring system[16] (calcd 16.4 Hz, Figure 4). Additionally, the coupling constants for the series are

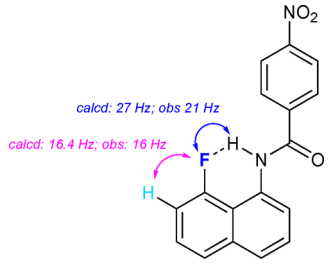

Figure 4. Major coupling constants observed experimentally and predicted by B3LYP/6-311++G** (compound **3**).

predicted to show a slight increase as the substituent on the benzene ring becomes more electron withdrawing (from 24.7 Hz for p-NMe_2 to 27 Hz for p-NO_2). However, this modest trend is not clearly discernible in the actual ^{19}F NMR data primarily due to the complex nature of the multiplets.

We then conducted an IR analysis of the NH···F interactions. It is generally accepted that the increasing strength of a classical hydrogen bond results in lengthening of the donor−H bond and an attendant shortening of the acceptor−H distance, inducing a red shift in the IR-stretching frequency.[26−30] An initial DFT analysis (ωB97XD/6-311+G**) of the synthesized molecules predicts a similar trend for NH stretches in the IR as the nature of substituent becomes more electron withdrawing, a possible indication of increasing hydrogen bond strength (Table 1).

The NH stretch in the experimentally observed IR spectra of the derivatives shows a continuous high energy shift as the aromatic ring becomes more electron deficient. The NH stretch of p-NO_2 derivative appears at 3470.5 cm^{-1}, which is ca. 16 cm^{-1} red-shifted compared to the same stretch in the p-NMe_2

https://dx.doi.org/10.1021/acs.joc.0c00553
J. Org. Chem. 2020, 85, 6195−6200

Table 1. Calculated (Scaled) and Experimentally Observed NH Stretching Frequencies in 1 through 4

NH stretch (cm^{-1})	R = NMe_2	OMe	H	NO_2
predicted	3517	3516	3503	3501
experimental	3486	3482	3477	3471

derivative, thus implying a significantly stronger H bond in the former case (Table 1 and Figure 5). Although substituent effects

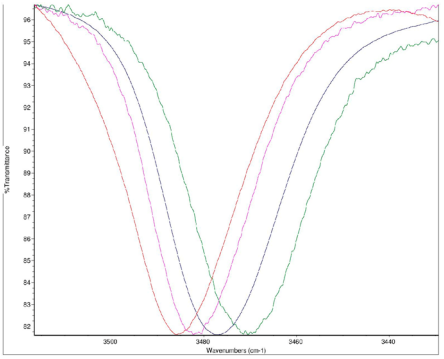

Figure 5. Experimentally observed NH stretches in IR spectra: red (p-NMe_2), purple (p-OMe), blue (p-H), green (p-NO_2).

have a relatively smaller effect on high energy shifts in the NH stretching frequency of benzamides, this fact does not necessarily imply a weak substituent effect on the hydrogen bond strength itself since the high energy shift in IR is considered only a semiquantitative measure.[31]

X-ray crystallographic analysis gives additional insight into the influence of fluorine substitution on crystal packing. We recently reported the crystal structure of a substituted trityl fluoride that is significantly different than the corresponding trityl hydride, confirming the inability of fluorine to act as an "isostere" for hydrogen when it comes to directionality/ordering.[32] Single crystal X-ray analysis of the p-NO_2 derivative **3** reveals an interesting feature: the naphthalene rings are aligned face to face in a $\pi-\pi$ interaction (Figure 6), which is significantly different than the crystal structure of *N*-(naphthalen-1-yl)benzamide, wherein the phenyl ring engages in T-shaped $\pi-\pi$ interactions with the naphthalene ring system.[33] This motif results in the formation of naphthalene-based sheets held by intermolecular hydrogen bonding between the amide N−H and a neighboring molecule's carbonyl oxygen at 2.12 Å. Moreover, the NH···F and

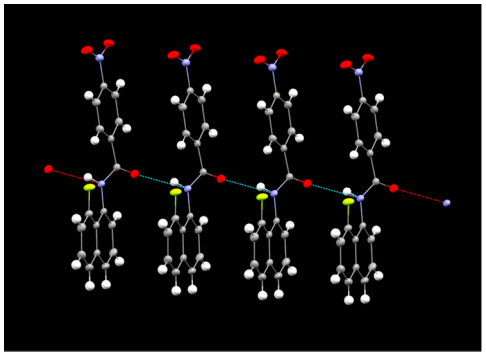

Figure 6. X-ray crystal structure of p-NO_2 benzamide derivative (**3**) with extended hydrogen bonding network forming sheets of naphthalene rings.

N−H distances of 2.22 and 0.87 Å are observed in the crystal structure of p-NO_2 benzamide derivative (Figure 6, see SI for details).

Finally, we imagined that an even larger high energy IR shift could be observed if the substituent is more electron withdrawing than p-NO_2Ph. A DFT analysis predicted that replacing the benzamide derivatives with trifluoroacetamide would show a significant red shift of an additional 39 cm^{-1} in NH stretching frequency compared to p-NO_2Ph derivative. In fact, when 8-fluoro-1-aminonaphthalene is acetylated with trifluoroacetic anhydride (Scheme 2, 86%), the NH stretch of

Scheme 2. Synthesis of the Trifluoroacetamide Derivative 11

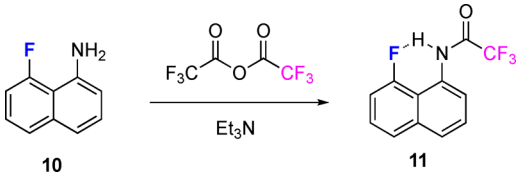

10 **11**

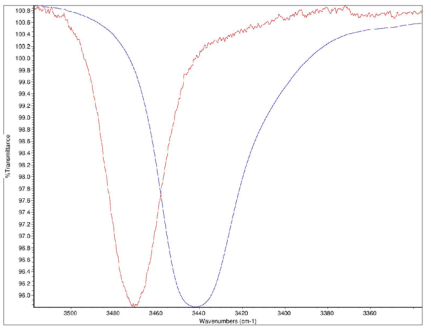

Figure 7. Experimentally observed NH stretches in IR spectra: red (p-NO_2Ph) peak at 3470.5 cm^{-1}, blue (CF_3) peak at 3442.9 cm^{-1}.

the product appears at 3443 cm^{-1}, red-shifted by 28 cm^{-1} compared to the p-NO_2 derivative (Figure 7). Additionally, its ^{19}F NMR spectrum shows a multiplet corresponding to aromatic fluorine with a spin−spin coupling constant of 19.1 Hz to the proximate N−H, even larger than that observed in **3**.

Single crystal X-ray analysis of the trifluoroacetamide derivative **11** also reveals an interesting structure. Similar to the benzamide derivatives, the crystal is characterized by sheets and bifurcated C−F···HN bonding with an amide carbonyl oxygen and fluorine on position 8 of the naphthalene ring (NH···F, 2.12 Å), (NH···O, 2.19 Å), (N−H···F_3C, 2.25 Å). Another interesting feature of trifluorobenzamide derivative's crystal structure is the close F···F distance (2.98 Å) between the CF_3 groups on adjacent molecules (Figure 8).

The X-ray crystal structures of **3** and **11**, however, depict amide NH···F distances of 2.22 and 2.12 Å, respectively, which are greater than the shortest NH···F distance found in the CCD and our predicted gas phase distances. This increased distance in the crystal structures can be attributed to intermolecular hydrogen bonding with neighboring molecule's carbonyl oxygen. In dilute solutions, however, we conclude that the intramolecular NH···F interaction dominates and the distance could be approximated to, or even smaller than, 1.93 Å. We optimized a few of the structures with the shortest NH···F distances reported in the CCD[34−37] at ωB97XD/6-311+G**

https://dx.doi.org/10.1021/acs.joc.0c00553
J. Org. Chem. 2020, 85, 6195−6200

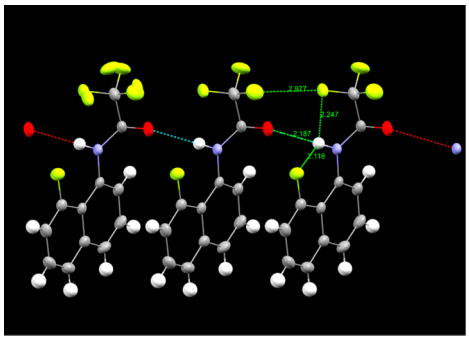

Figure 8. X-ray crystal structure of trifluoroacetamide derivative **11** depicting an extended hydrogen bonding network forming sheets of naphthalene rings.

and calculated spin−spin coupling constants for the NH···F interactions therein at B3LYP/6-311++G** (see SI for structures and computational details). DFT calculations predict an inverse correlation of the NH···F coupling constants and distances between the interacting nuclei (Figure 9). The largest

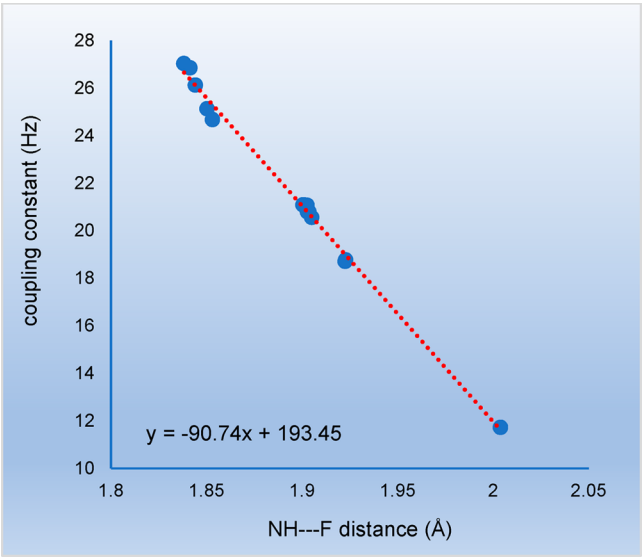

Figure 9. Correlation between calculated NH···F distances and corresponding coupling constants calculated at B3LYP/6-311++G** using molecules **1**−**4** and **11**−**20**. See SI for details.

amide NH···F coupling constant reported in the literature is 17.1 Hz.[35] This is smaller than those observed in our molecules which are, both predicted and experimentally, more than 20 Hz, indicating the *possibility* of an amide NH···F distance shorter than those observed so far. The trend in Figure 9 predicts NH···F distances in the series of our benzamide derivatives to be approximately 1.90 Å in dilute solutions, in line with DFT geometry calculations. However, when it comes to crystal packing, the NH proton skews out of the plane of naphthalene ring as a result of competitive intermolecular NH···OC hydrogen bonding.

CONCLUSION

In this note, we have synthesized a series of *N*-(8-fluoronaphthalen-1-yl)benzamide derivatives and established a correlation between the strength of NH···F hydrogen bonding interaction and substituents on the benzamide ring. Both ^{1}H and ^{19}F NMR spectra indicate the exclusive formation of the desired geometry, attributed to the favorable hydrogen bonding interactions, most notably through strong spin−spin coupling of H and F. Moreover, IR analysis of the series predicts a direct correlation between the electron withdrawing nature of substituents and the hydrogen bond strength. X-ray crystallographic analysis reveals the formation of sheets characterized by face-to-face $\pi-\pi$ interactions between the naphthalene rings. We hope that these results provide additional insights into the increasingly important role of fluorine in hydrogen bonding interactions.

EXPERIMENTAL SECTION

^{1}H and ^{13}C spectra were acquired on a 400 MHz NMR in $CDCl_3$ at 25 °C, while ^{19}F spectra were acquired on a 300 MHz NMR in $CDCl_3$. The ^{1}H, ^{13}C, and ^{19}F chemical shifts are given in parts per million (δ) with respect to an internal tetramethylsilane (TMS, δ 0.00 ppm) standard. NMR data are reported in the following format: chemical shifts (multiplicity (s = singlet, d = doublet, t = triplet, q = quartet, m = multiplet), coupling constants [Hz], integration). IR data were obtained using an FT-IR with a flat CaF_2 cell. HRMS data were obtained on a Thermo Scientific Q-Exactive Orbitrap mass spectrometer.

General Protocol for Synthesis of the *N*-(8-Fluoronaphthalen-1-yl)benzamide Derivatives. To a solution of **10** in 10 mL CH_2Cl_2, 1 equiv of the appropriate benzoyl chloride derivative was added at room temperature. To the mixture, 0.1 mL Et_3N was added and the solution was stirred at room temperature for 2 h. The solvent was evaporated under reduced pressure and the desired product was purified with MPLC using hexanes and ethyl acetate as eluents.

*N-(8-Fluoronaphthalen-1-yl)-4-methoxybenzamide (Compound **1**).* Compound **1** was synthesized following the general protocol for benzamide derivative synthesis and isolated as colorless crystalline solid (135 mg, 75% isolated yield). ^{1}H NMR ($CDCl_3$) δ 9.6 (d, J = 20.6 Hz, 1H), 8.76 (d, J = 7.7 Hz, 1H), 7.94 (d, J = 8.7 Hz, 1H), 7.5−7.66 (m, 3H), 7.3−7.4 (m, 1H), 7.1−7.2 (m, 1H), 7.01 (d, J = 8.7 Hz, 1H), 3.88 (s, 3H); ^{13}C NMR {^{1}H} ($CDCl_3$) δ 165, 164.97, 165.5, 160.3, 157.9, 136.6, 136.5, 132.93, 132.89, 128.8, 127.4, 127.30, 127.29, 125.56, 125.46, 125.41, 125.38, 123.70, 123.67, 118.32, 118.30, 115.05, 114.97, 114.1, 111.3, 111.1, 55.5; ^{19}F NMR ($CDCl_3$) δ −117 (m, 1F); ^{19}F NMR {^{1}H} ($CDCl_3$) δ −117 (s, 1F); IR 3482, 1675, 1606, 1537, 1495, 1432, 1341 (cm^{-1}, CaF_2, CH_2Cl_2); FTMS (ESI) m/z [M + H]$^+$ Calcd for $C_{18}H_{15}FNO_2^+$ 296.1081, found 296.1076.

*N-(8-Fluoronaphthalen-1-yl)benzamide (Compound **2**).* Compound **2** was synthesized following the general protocol for benzamide derivative synthesis and isolated as a light pink solid (145 mg, 80% isolated yield). ^{1}H NMR ($CDCl_3$) δ 9.69 (d, J = 20.8 Hz, 1H), 8.73 (d, J = 7.86 Hz, 1H), 8.38 (m, 2H), 8.13 (m, 2H), 7.7 (m, 2H), 7.5−7.6 (t, J = 8 Hz, 1H), 7.4−7.47 (m, 1H), 7.19−7.25 (m, 1H); ^{13}C NMR {^{1}H} ($CDCl_3$) δ 163.3, 160.1, 157.7, 149.8, 140.7, 136.51, 136.48, 131.95, 131.91, 128.1, 127.23, 127.21, 125.93, 125.82, 125.62, 125.59, 124.81, 124.79, 124.2, 118.91, 118.89, 150.07, 149.99, 111.7, 111.5; ^{19}F NMR ($CDCl_3$) δ −116.96 (m, 1F); ^{19}F NMR {^{1}H} ($CDCl_3$) δ −116.96 (s, 1F); IR 3477, 1681, 1541, 1487, 1432, 1342 (cm^{-1}, CaF_2, CH_2Cl_2); FTMS (ESI) m/z [M + H]$^+$ Calcd for $C_{17}H_{13}FNO^+$ 266.0976, found 266.0970.

*N-(8-Fluoronaphthalen-1-yl)-4-nitrobenzamide (Compound **3**).* Compound **3** was synthesized following the general protocol for benzamide derivative synthesis and isolated as a yellow solid (162 mg, 85% isolated yield). ^{1}H NMR ($CDCl_3$) δ 9.7 (d, J = 21 Hz, 1H), 8.79 (m, 1H), 7.98 (m, 1H), 7.5−7.68 (m, 6H), 7.34−7.42 (m, 1H), 7.15−7.23 (m, 1H); ^{13}C NMR {^{1}H} ($CDCl_3$) δ 165.45, 165.43, 160.3, 157.8, 136.55, 136.51, 135.2, 132.72, 132.68, 131.9, 128.9, 127.30, 127.29, 126.9, 125.6, 125.5, 125.44, 125.40, 123.98, 123.95, 118.49, 118.47, 115.1, 115, 111.4, 111.2; ^{19}F NMR ($CDCl_3$) δ −117 (m, 1F); ^{19}F NMR {^{1}H} ($CDCl_3$) δ −117 (s, 1F); IR 3470, 1688, 1606, 1540, 1531, 1503, 1487, 1347 (cm^{-1}, CaF_2, CH_2Cl_2); FTMS (ESI) m/z [M + H]$^+$ Calcd for $C_{17}H_{12}FN_2O_3^+$ 311.0826, found 311.0819.

https://dx.doi.org/10.1021/acs.joc.0c00553
J. Org. Chem. 2020, 85, 6195−6200

Synthesis of 4-(Dimethylamino)-*N*-(8-fluoronaphthalen-1-yl)benzamide (Compound 4). Compound **3** (100 mg, 0.32 mmol) was dissolved in 30 mL EtOH:THF (2:1) and Pd/C was added to the solution. The mixture was purged with H_2 gas until TLC indicated complete consumption of **3** and the mixture was purged with excess H_2 gas for another 30 min. Pd/C was then filtered through Celite and the cake was washed with 15 mL THF. The solvent was evaporated under reduced pressure and the ^{1}H NMR of mixture indicated complete conversion of NO_2 to NH_2. The intermediate p-NH_2 derivative was utilized without further purification. It was dissolved in 20 mL EtOH, 200 mg (1.45 mmol) of K_2CO_3 and 0.1 mL (1.6 mmol) MeI were added to the mixture and the solution was refluxed overnight. The reaction mixture was filtered over Celite, washed with 10 mL EtOH, and filtrate was evaporated under reduced pressure. The dimethylated product was isolated by MPLC using hexanes and ethyl acetate as eluent as a light pink solid (35 mg, 35% isolated yield). ^{1}H NMR ($CDCl_3$) δ 9.63 (d, J = 21.1 Hz, 1H), 8.82 (m, 1H), 7.88 (m, 2H), 7.5−7.67 (m, 3H), 7.3−7.41 (m, 1H), 7.12−7.22 (m, 1H), 6.76 (m, 2H), 3.06 (s, 6H); ^{13}C NMR {^{1}H} ($CDCl_3$) δ 165.49, 165.47, 160.5, 158.1, 152.7, 136.62, 136.58, 128.5, 127.42, 127.40, 125.42, 125.38, 125.35, 125.32, 123.17, 123.14, 121.8, 117.97, 117.95, 114.98, 114.90, 111.3, 111.2, 110.9, 40.1; ^{19}F NMR ($CDCl_3$) δ −116.29 (m, 1F); ^{19}F NMR {^{1}H} ($CDCl_3$) δ −116.29 (s, 1F); IR 3486, 1669, 1607, 1541, 1526, 1501 (cm^{-1}, CaF_2, CH_2Cl_2); FTMS (ESI) m/z $[M + H]^+$ Calcd for $C_{19}H_{18}FN_2O^+$ 309.1398, found 309.1392.

Synthesis of 2,2,2-Trifluoro-*N*-(8-fluoronaphthalen-1-yl)-acetamide (Compound 11). To a solution of **10** (110 mg, 0.68 mmol) in 10 mL DCM was added 0.1 mL (0.7 mmol) of trifluoroacetic anhydride and 0.1 mL Et_3N. After stirring at room temperature for 2 h, the solvent was evaporated under reduced pressure and the product was purified on MPLC using hexanes and ethyl acetate as eluents as a white solid (150 mg, 86% isolated yield). ^{1}H NMR ($CDCl_3$) δ 9.7 (d, J = 19.9 Hz, 1H), 8.52 (m, 1H), 7.6−7.8 (m, 2H), 7.5−7.59 (m, 1H), 7.4−7.49 (m, 1H), 7.15−7.3 (m, 1H); ^{13}C NMR {^{1}H} ($CDCl_3$) δ 159.7, 157.3, 155, 154.6, 136.31, 136.28, 129.74, 129.70, 126.96, 126.94, 126.3, 126.2, 125.97, 125.94, 125.50, 125.46, 120.1, 119.36, 119.34, 117.3, 115.0, 114.9, 114.4, 112.1, 111.9; ^{19}F NMR ($CDCl_3$) δ −117.9 (m, 1F), −76.19 (s, 3F); IR 3443, 1737, 1638, 1555, 1507, 1443, 1382 (cm^{-1}, CaF_2, CH_2Cl_2); FTMS (ESI) m/z $[M + H]^+$ Calcd for $C_{12}H_8F_4NO^+$ 258.0536, found 258.0530.

■ ASSOCIATED CONTENT

Supporting Information

The Supporting Information is available free of charge at https://pubs.acs.org/doi/10.1021/acs.joc.0c00553.

Crystal Structure of Compound **3** (CCDC 1987532) (CIF)

Crystal Structure of Compound **11** (CCDC 1987533) (CIF)

NMR spectra, crystal structure data, and computational information (PDF)

■ AUTHOR INFORMATION

Corresponding Author

Thomas Lectka − *Department of Chemistry, Johns Hopkins University, Baltimore, Maryland 21218, United States;* orcid.org/0000-0003-3088-6714; Email: lectka@jhu.edu

Authors

Muhammad Kazim − *Department of Chemistry, Johns Hopkins University, Baltimore, Maryland 21218, United States;* orcid.org/0000-0003-2020-8952

Maxime A. Siegler − *Department of Chemistry, Johns Hopkins University, Baltimore, Maryland 21218, United States;* orcid.org/0000-0003-4165-7810

Complete contact information is available at: https://pubs.acs.org/10.1021/acs.joc.0c00553

Notes

The authors declare no competing financial interest.

■ ACKNOWLEDGMENTS

T.L. thanks the National Science Foundation (Grant CHE 1800510) for financial support. Mass spectral data were obtained at University of Delaware's mass spectrometry center.

■ REFERENCES

(1) Vishnumurthy, K.; Guru Row, T. N.; Venkatesan, K. Fluorine in Crystal Engineering: Photodimerization of (1*E*,3*E*)-1-phenyl-4-pentafluorophenylbuta-1,3-dienes in the Crystalline State. *Photoch. PhotoBio. Sci.* **2002**, *6*, 427−430.

(2) Kawahara, S.; Tsuzuki, S.; Uchimaru, T. Theoretical Study of the C-F// Interaction: Attractive Interaction Between Fluorinated Alkane and an Electron-Deficient:-System. *J. Phys. Chem. A* **2004**, *108*, 6744−6749.

(3) Jackel, C.; Koksch, B. Fluorine in Peptide Design and Protein Engineering. *Eur. J. Org. Chem.* **2005**, *21*, 4483−4503.

(4) Riley, K. E.; Merz, K. M. Effects of Fluorine Substitution on the Edge-to-Face Interaction of Benzene Dimer. *J. Phys. Chem. B* **2005**, *109*, 17752−17756.

(5) Chopra, D.; Nagarajan, K.; Guru Row, T. N. Analysis of Weak Interactions Involving Organic Fluorine: Insights From Packing Features in Substituted 4-Keto-tetrahydroindoles. *J. Mol. Struct.* **2008**, *888*, 70−83.

(6) Zhou, P.; Zou, J.; Tian, F.; Shang, Z. Fluorine Bonding − How Does It Work In Protein − Ligand Interactions? *J. Chem. Inf. Model.* **2009**, *49*, 2344−2355.

(7) Struble, M. D.; Guan, L.; Siegler, M. A.; Lectka, T. A C−F Bond Directed Diels−Alder Reaction. *J. Org. Chem.* **2016**, *81*, 8087−8090.

(8) Holl, M. G.; Struble, M. D.; Singal, P.; Siegler, M. A.; Lectka, T. Positioning a Carbon-Fluorine Bond Over the Cloud of an Aromatic Ring: A Different Type of Arene Activation. *Angew. Chem., Int. Ed.* **2016**, *55*, 8266−8269.

(9) Struble, M. D.; Kelly, C.; Siegler, M. A.; Lectka, T. Search for a Strong, Virtually "No Shift" Hydrogen Bond: A Cage Molecule with an Exceptional OH—F Interaction. *Angew. Chem., Int. Ed.* **2014**, *53*, 8924−8928.

(10) Holl, M. G.; Pitts, C. R.; Lectka, T. Quest for a Symmetric [C−F−C]$^+$ Fluoronium Ion in Solution: A Winding Path to Ultimate Success. *Acc. Chem. Res.* **2020**, *53*, 265−275.

(11) Pitts, C. R.; Siegler, M. A.; Lectka, T. Intermolecular Aliphatic C−F—H−C Interaction in the Presence of "Stronger" Hydrogen Bond Acceptors: Crystallographic, Computational, and IR Studies. *J. Org. Chem.* **2017**, *82*, 3996−4000.

(12) Holl, M. G.; Struble, M. D.; Siegler, M. A.; Lectka, T. The Close Interaction of a C−F Bond with a Carbonyl F-System: Attractive, Repulsive, or Both? *J. Fluorine Chem.* **2016**, *188*, 126−130.

(13) Holl, M. G.; Pitts, C. R.; Lectka, T. Fluorine in a C−F Bond as the Key to Cage Formation. *Angew. Chem., Int. Ed.* **2018**, *57*, 2758−2766.

(14) Zhu, W.; Yang, W.; Zhou, W.; Liu, H.; Wei, S.; Fan, J. A. New Crystal Structure and Fluorescence Property of N-2-Fluorobenzoyl-N'-4-tolylthiourea. *J. Mol. Struct.* **2011**, *1004*, 74−81.

(15) Cox, C.; Wack, H.; Lectka, T. Strong Hydrogen Bonding to the Amide Nitrogen Atom in an "Amide Proton Sponge": Consequences for Structure and Reactivity. *Angew. Chem., Int. Ed.* **1999**, *38*, 798−800.

(16) Scerba, M. T.; Leavitt, C. M.; Diener, M. E.; DeBlase, A. F.; Guasco, T. L.; Siegler, M. A.; Bair, N.; Johnson, M. A.; Lectka, T. NH$^+$−F Hydrogen Bonding in a Fluorinated "Proton Sponge" Derivative: Integration of Solution, Solid-State, Gas-Phase, and Computational Studies. *J. Org. Chem.* **2011**, *76*, 7975−7984.

(17) Alder, R. W.; Bowman, P. S.; Steele, W. R. S.; Winterman, D. R. The Remarkable Basicity of 1,8-Bis(dimethylamino)naphthalene. *Chem. Commun.* **1968**, *13*, 723−724.

(18) Staab, H. A.; Saupe, T. Proton Sponges" and the Geometry of Hydrogen Bonds: Aromatic Nitrogen Bases with Exceptional Basicities. *Angew. Chem., Int. Ed. Engl.* **1988**, *27*, 865−879.
(19) Alder, R. W. Strain Effects on Amine Basicities. *Chem. Rev.* **1989**, *89*, 1215−1223.
(20) Hibbert, F.; Emsley, J. Hydrogen Bonding and Chemical Reactivity. *Adv. Phys. Org. Chem.* **1990**, *26*, 255−379.
(21) Hunter, C. A.; Sanders, J. K. M. The Nature of Interactions. *J. Am. Chem. Soc.* **1990**, *112*, 5525−5534.
(22) Hunter, C. A.; Singh, J.; Thornton, J. M. Interactions: The Geometry and Energetics of Phenylalanine-Phenylalanine Interactions in Proteins. *J. Mol. Biol.* **1991**, *218*, 837−846.
(23) Martinez, C. R.; Iverson, B. L. Rethinking the Term "pi-stacking. *Chem. Sci.* **2012**, *3*, 2191−2201.
(24) Malathy Sony, S. M.; Ponnuswamy, M. N. Nature of Interactions in Nitrogen-Containing Heterocyclic Systems: A Structural Database Analysis. *Cryst. Growth Des.* **2006**, *6*, 736−742.
(25) Zhu, Z.; Colbry, N. L.; Lovdahl, M.; Mennen, K. E.; Acciacca, A.; Beylin, V. G.; Clark, J. D.; Belmont, D. T. Practical Alternative Synthesis of 1-(8-Fluoro-naphthalen-1-yl-)piperazine. *Org. Process Res. Dev.* **2007**, *11*, 907−909.
(26) Arunan, E.; Desiraju, G. R.; Klein, R. A.; Sadlej, J.; Scheiner, S.; Alkorta, I.; Clary, D. C.; Crabtree, R. H.; Dannenberg, J. J.; Hobza, P.; Kjaergaard, H. G.; Legon, A. C.; Mennucci, B.; Nesbitt, D. J. Definition of the Hydrogen Bond (IUPAC Recommendations 2011). *Pure Appl. Chem.* **2011**, *83*, 1637−1641.
(27) Joseph, J.; Jemmis, E. D. Red-, Blue- or No-Shift in Hydrogen Bonds: A Unified Explanation. *J. Am. Chem. Soc.* **2007**, *129*, 4620−4632.
(28) Duarte, L. J.; Silva, A. F.; Richter, W. E.; Bruns, R. E. Infrared Intensification and Hydrogen Bond Stabilization: Beyond Point Charges. *J. Phys. Chem. A* **2019**, *123*, 6482−6490.
(29) Mao, Y.; Head-Gordon, M. Probing Blue-Shifting Hydrogen Bonds with Adiabatic Energy Decomposition Analysis. *J. Phys. Chem. Lett.* **2019**, *10*, 3899−3905.
(30) Wang, C.; Mo, Y. Classical Electrostatic Interaction is the Origin for Blue-Shifting Halogen Bonds. *Inorg. Chem.* **2019**, *58*, 8577−8586.
(31) Rozenberg, M.; Loewenschuss, A.; Marcus, Y. An Empirical Correlation Between Stretching Vibration Redshift and Hydrogen Bond Length. *Phys. Chem. Chem. Phys.* **2000**, *2*, 2699−2702.
(32) York, G. D.; Siegler, M. A.; Patel, D. D.; Lectka, T. Synthesis and X-Ray Crystallography of a Substituted Trityl Fluoride: Ordering Power of a C−F Bond. *J. Fluorine Chem.* **2019**, *228*, 109377.
(33) Zhu, R.; Ren, Y.; Li, W. *N*-(Napthalen-1-yl)benzamide. *Acta Crystallogr., Sect. E: Struct. Rep. Online* **2011**, *E67*, No. o3204.
(34) Zhao, X.; Wang, X. Z.; Jiang, X. K.; Chen, Y. Q.; Li, Z. T.; Chen, G. J. Hydrazide-Based Quadruply Hydrogen-Bonded Heterodimers. Structure, Assembling Selectivity, and Supramolecular Substitution. *J. Am. Chem. Soc.* **2003**, *125*, 15128−15139.
(35) Li, C.; Ren, S. F.; Hou, J. L.; Yi, H. P.; Zhu, S. Z.; Jiang, X. K.; Li, Z. T. F—H−N Hydrogen Bonding Driven Foldamers: Efficient Receptors for Dialkylammonium Ions. *Angew. Chem., Int. Ed.* **2005**, *44*, 5725−5729.
(36) Zhu, K. Y.; Wu, J.; Li, C.; Zhu, J.; Hou, J. L.; Li, C. Z.; Jiang, X. K.; Li, Z. T. F—H−N and MeO—H−N Hydrogen Bonding in the Solid States of Aromatic Amides and Hydrazides: A Comparison Study. *Cryst. Growth Des.* **2007**, *7*, 1490−1496.
(37) Bhandary, S.; Gonde, S.; Chopra, D. Dissecting the Conformational and Interaction Topological Landscape of *N*-ethynylphenylbenzamide by the Device of Polymorphic Diversity. *Cryst. Growth Des.* **2019**, *19*, 1072−1085.

https://dx.doi.org/10.1021/acs.joc.0c00553
J. Org. Chem. 2020, 85, 6195−6200